PERIODICA POLYTECHNICA SER. EL. ENG. VOL. 35, NO. 4, PP. 285-292 (1991)

HIGH ACCURACY RADAR CROSS SECTION MEASUREMENTS AT 3–18 GHz

S. MIHÁLY, D. KÄHNY*, I. BOZSÓKI and W. WIESBECK*

*Institut für Höchstfrequenztechnik und Elektronik
Universität Karlsruhe

Department of Microwave Telecommunications
Technical University, Budapest

Received: April 20, 1991.
Revised: Dec. 12, 1991.

Abstract

A microwave network-analyzer based Radar Cross Section (RCS) measuring set-up is described with calibration method developed at the Institut für Höchstfrequenztechnik und Elektronik, Universität Karlsruhe. High-accuracy RCS data can be obtained by the system in the 3–18 GHz microwave band.

A series of examples is given in the form of corner- reflector test-measurements.

Keywords: microwave backscattering, radar cross section, cross polarized scattering.

Introduction

Accurate microwave radar cross sections (RCS) of various targets are widely-needed measurement data. This parameter gives the relationship between the incident and scattered electric field upon a target at a given frequency, polarization and direction of incidence and scattering (RIEGGER – WIESBECK, 1986).

One application of RCS data measured in laboratory conditions is calibration of reference targets for imaging microwave sensors, like radars (BACHMAN, 1982 and CURRIE, 1984). Beside this, gaining reliable experimental information about scattering properties of individual scattering elements of a complex target (e. g. tree or any vegetation layer) could help in theoretical modelling of microwave backscattering characteristics of complex structures, which is essential for the correct interpretation of images based on microwave reflectivity of the object viewed by a microwave sensor (KRUL, 1981, MIHÁLY – BOZSÓKI, 1988).

This kind of problem frequently occurs in microwave remote sensing, the techniques of obtaining information on distant targets without any physical contact, simply relying on the backscattered microwave signal, originally emitted by the microwave remote sensing instrument (TREVETT, 1986).

Network Analyzer Based Set-Up

The description of the set-up is illustrated in *Fig. 1.* The main block of the RCS measuring system is a Vector Network-analyzer (VNwa) consisting of a synthesizer with sweep capability up to 26.5 GHz, a four channel phase- locked receiver and two closely positioned, orthogonally polarized wideband antennas (quasi monostatic mesurement). The horizontal or the vertical input of the transmitting antenna is fed alternately, the two orthogonal channels of the receiving antenna are simultaneously connected to the VNwa. The fourth channel of the receiver can be used either for transmission or attenuation measurement.

The measurements are carried out in an anechoic chamber, but can be performed in other environments as well due to the used excellent calibration procedure. The whole system is controlled by a HP 9000/320 computer.

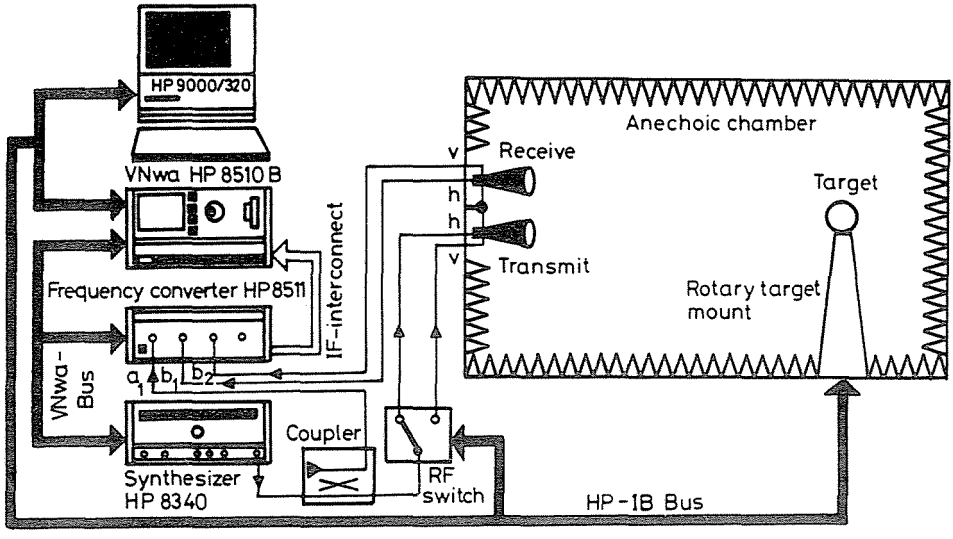

Fig. 1. Network-analyzer based set-up

Measurement Errors and Calibration Algorithm

There are three main categories of systematic errors occurring in a polarimetric measurement set-up.

— Finite RF-absorption of the anechoic chamber and leakage between the two antennas;
— Frequency-response error due to the RF-components;
— Direct coupling between vertical and horizontal channel in the transmit or receive antenna limiting the measurement accuracy of co-polarized components.

Commonly, the polarization properties are characterized using the cross polarization scattering matrix, that combines the incident electric field at the target, which is assumed to be a plane-wave, and the field at the receiving antenna.

$$\begin{bmatrix} E_h^r \\ E_v^r \end{bmatrix} = \begin{bmatrix} S_{hh} & S_{hv} \\ S_{vh} & S_{vv} \end{bmatrix} \begin{bmatrix} E_h^i \\ E_v^i \end{bmatrix} . \tag{1}$$

E^i: Incident electric field at the target;
E^r: Scattered electric field at the antenna.

The systematic errors described above can be quantified by 20 complex error coefficients in the following matrix equation which relate the measured (incorrect) and the calculated (error-free) target scattering parameters:

$$\begin{bmatrix} S_{vv}^m \\ S_{hh}^m \\ S_{vh}^m \\ S_{hv}^m \end{bmatrix} = \begin{bmatrix} C_{10} \\ C_{20} \\ C_{30} \\ C_{40} \end{bmatrix} + \begin{bmatrix} C_{11} & C_{12} & C_{13} & C_{14} \\ C_{21} & C_{22} & C_{23} & C_{24} \\ C_{31} & C_{32} & C_{33} & C_{34} \\ C_{41} & C_{42} & C_{43} & C_{44} \end{bmatrix} \begin{bmatrix} S_{vv}^0 \\ S_{hh}^0 \\ S_{vh}^0 \\ S_{hv}^0 \end{bmatrix} . \tag{2}$$

S^m: Measured values;
S^0: Correct (calculated) values.

These twenty error coefficients may be determined by a set of four, linear, independent calibration measurements. The complex polarization matrix of the reference objects must be known completely. The calibration targets are

— Empty room;
— Sphere;
— Dihedral corner reflector, first aspect angle;
— Dihedral corner reflector, second aspect angle.

The empty room measurement eliminates system errors caused by the mutual coupling of the antennas and residual reflections of the anechoic

chamber. The sphere is an ideal calibration target because it can be manufactured precisely and its theoretical RCS is calculated without approximation. Additionally it reflects no cross-polarized signal. The corner-reflector is used twice. In the first position it does not depolarize incident fields. In the second step it is rotated 45 degrees into the position of maximum cross polarization.

Fig. 2 shows the HH and HV RCS of a sphere with 36 mm diameter in the frequency-domain after calibration. The corresponding time-domain plot of the HH RCS is plotted in *Fig. 3*.

The frequency-domain curves show the familiar resonance region for the like-polarised data, and extremely low RCS for cross polarization. The time-domain curves can be interpreted as the reflection of the direct wave from the nearest specular point of the sphere, and the creeping wave, coming from after a turn-around, with a delay of half the circumference plus twice the radius of the sphere, measured in free-space.

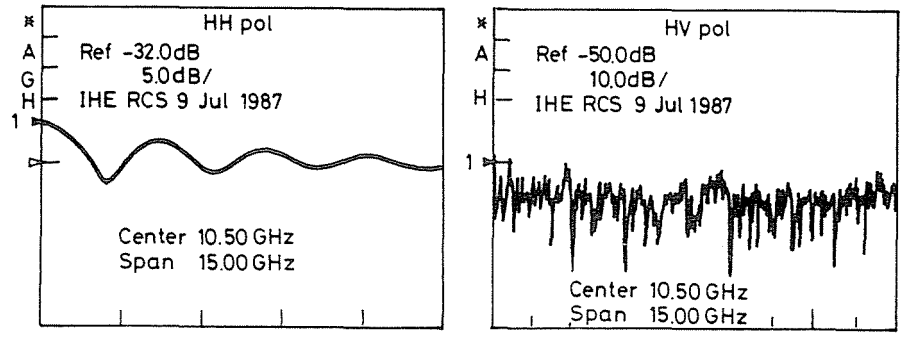

Fig. 2. Frequency domain RCS curves of a 36 mm diameter sphere

RCS Measurement of Reference Corner Reflectors

The first series of measurements demonstrates the behaviour of a simply manufactured corner-reflector. For getting a reference-reflector a plane hexagon has also been manufactured, having the same reflecting surface as that of the 200 mm corner-reflector.

Fig. 4 gives the RCS of the reference plane-reflector in the frequency-domain. In this frequency-range the curve corresponds very precisely to the values, which are obtained from the geometric-optics approach of the RCS of a plane-target, see (3).

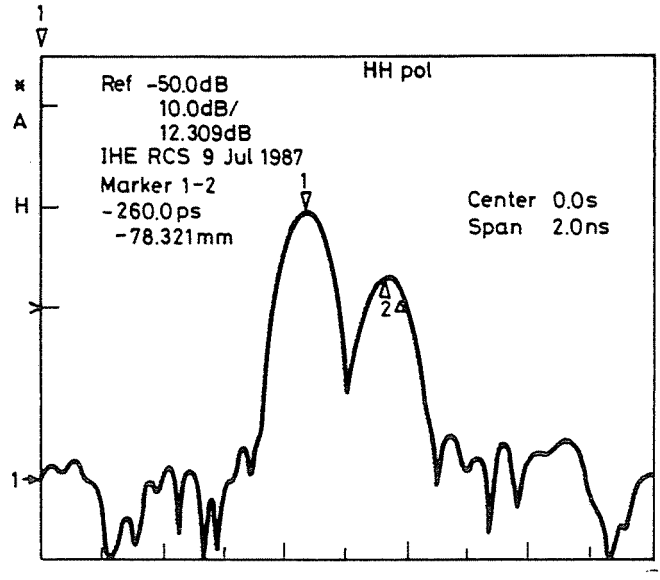

Fig. 3. Time-domain HH RCS of a 36 mm diameter sphere

$$\sigma = 4\pi \frac{A^2}{\lambda^2} . \tag{3}$$

σ — RCS at perpendicular incidence and scattering;
A — geometric area of plane target;
λ — wavelength of incident electromagnetic wave.

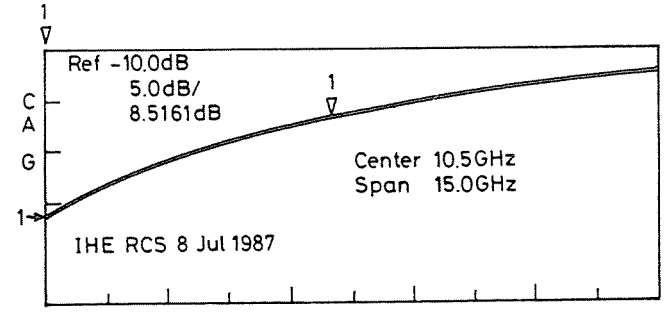

Fig. 4. Frequency-domain RCS of a reference hexagonal plane-reflector

Fig. 5 shows the frequency-domain RCS of a corner-reflector, which has a 200 mm long edge on the side. As it is clearly seen the latter characteristic does not follow what one would expect, namely an identical curve to *Fig. 4*. The main reason why the very large difference occurs is that it is not only the virtual plane at the back-tip of the corner parallel with the plane of the front-edges of the reflector which gives backscattering, but the front-edges themselves are also very good reflectors.

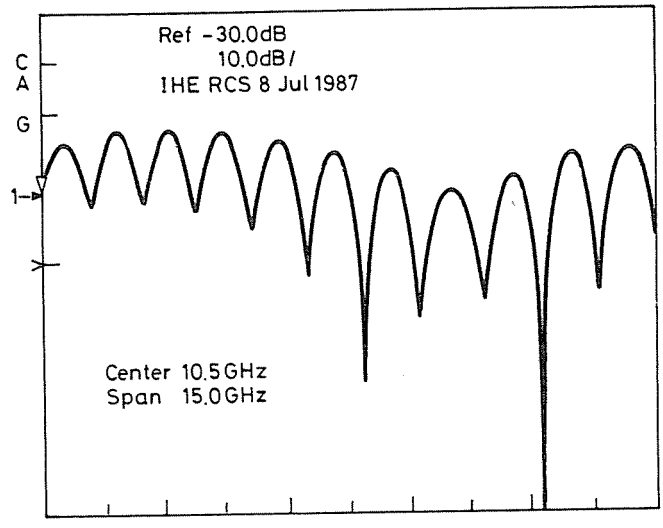

Fig. 5. Frequency-domain RCS of 200 mm corner-reflector

In *Fig. 6* the reflections of three targets are compared in the time-domain after taking the FFT transform of the frequency-domain RCS responses. Two of them were identical corner-reflectors, with 200 mm length at the shorter edge of the walls. The third target was a plane hexagon, producing the same reflecting area as that of the corner reflectors. It can be seen that both corner-reflectors have very similar RCS behaviour, both curves show the double reflection peaks, one from the edges and the other from the main reflecting plane. As a reference measurement the plane hexagon has been placed exactly in the plane of the corner edges, so it is clearly seen that a major part of the resulting reflection is from this plane.

A way of avoiding the strong edge-reflections is to make the reflector edges as narrow as possible (KÄHNY, 1990).

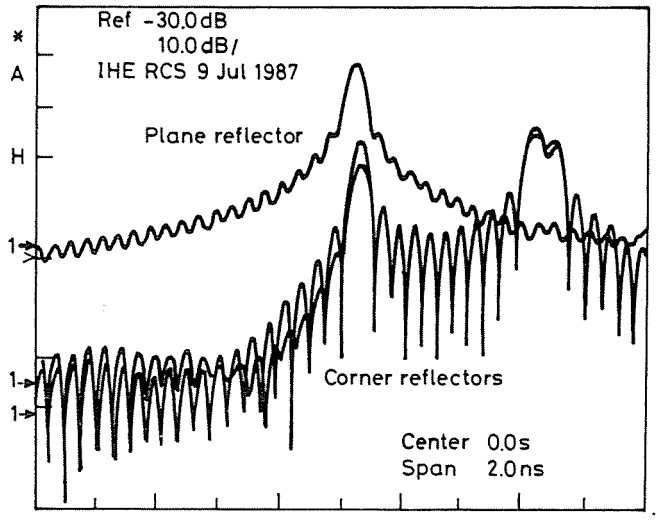

Fig. 6. Time-domain RCS of 200 mm corner-reflector

Conclusions

A microwave-band measurement set-up installed at IHE, Karlsruhe, with its calibration algorithm, developed at the same Institute has been discussed, which system is able to make very precise co- and cross-polarized measurement of RCS of various targets.

Measurements carried out at plane- and corner-reflectors have pointed out the usefulness of the time-domain and frequency-domain conversion facility in searching for different scattering centers of specific objects.

References

BACHMAN, C. G. (1982): Radar Targets, Lexington Books, Lexington.

CURRIE, N. C. (1984): Techniques of Radar Reflectivity Measurement, Artech House, Washington.

KÄHNY, D. – VAN ZYL, J. (1990): How Does Corner Reflector Construction Affect Polarimetric SAR-Calibration? *Proc. IGARSS Symposium,* Maryland, IEEE, 90CH2825-8, pp. 1093–1097.

KRUL, L. (1981): Scatterometer Systems, *Proc. ESA-EARSeL Workshop,* Alpbach, Austria, ESA SP-166, pp. 19–27.

MIHÁLY, S. – BOZSÓKI, I. (1988): X-Band Scatterometry in Agriculture, *Proc. IGARSS Symposium,* Edinburgh, ESA SP-284, pp. 1287–1290.

RIEGGER, S, – WIESBECK, W. (1986): Coherent Polarimetric RCS Measurement on Trees, *Proc. IGARSS Symposium,* Zürich, ESA SP-254, pp. 883–887.

TREVETT, J. W. (1986): Imaging Radar for Resources Surveys, Chapman and Hall, London.

Addresses:

Sándor MIHÁLY and Prof. Dr. István BOZSÓKI
Department of Microwave Telecommunications
Technical University of Budapest
1521 Budapest

Däniael KÄHNY and Prof. Dr. Werner WIESBECK
Institut für Höchstfrequenztechnik und Elektronik
Universität Karlsruhe
Kaiserstraße 12, 7500 Karlsruhe, Deutschland